Fish and Shellfish Immunology 94 (2019) 780–791

Contents lists available at ScienceDirect

Fish and Shellfish Immunology

journal homepage: www.elsevier.com/locate/fsi

Full length article

Transcriptome sequencing reveals phagocytosis as the main immune response in the pathogen-challenged sea urchin *Strongylocentrotus intermedius*

Weijie Zhang[a,c], Zhong Wang[c], Xiaofei Leng[d], Huijie Jiang[b], Lei Liu[c], Chenghua Li[a,b,*], Yaqing Chang[c,**]

[a] State Key Laboratory for Quality and Safety of Agro-products, Ningbo University, Ningbo, Zhejiang Province, 315211, PR China
[b] Laboratory for Marine Fisheries Science and Food Production Processes, Qingdao National Laboratory for Marine Science and Technology, Qingdao, 266071, PR China
[c] Key Laboratory of Mariculture & Stock Enhancement in North China's Sea, Ministry of Agriculture and Rural Affairs, Dalian Ocean University, Dalian, 116023, PR China
[d] Dalian Haibao Fishery, CO., Ltd, Dalian, 116041, PR China

ARTICLE INFO

Keywords:
Strongylocentrotus intermedius
Spotting disease
Artificial infection
Transcriptome
qPCR

ABSTRACT

The clarification of host immune responses to causative bacteria of spotting disease in the sea urchin *Strongylocentrotus intermedius* is vital to preventing and controlling this disease, especially to selective breeding for disease resistance. For this purpose, sea urchins were challenged with the causative bacterium *Vibrio* sp. to obtain spotting diseased and undiseased samples. We conducted next-generation sequencing to assess the key genes/pathways in control (CG), diseased (DG), and undiseased (UG) groups. A total of 454.1 million clean reads were obtained and assembled into 23,899 UniGenes with an N50 of 1359 bp, with 86.11% of them matching the genome sequence of the sea urchin *S. purpuratus*. A total of 8415 UniGenes were mapped to the non-redundant database. Salmon expression analysis revealed 725 significantly differentially expressed genes (DEGs) among CG, DG, and UG. These DEGs were enriched into 72 Kyoto Encyclopedia of Genes and Genomes (KEGG) pathways, including a core set of immune correlated pathways notably in the phagosome, vitamin digestion and absorption, Wnt signaling, and Notch signaling pathways. DG was evidently upregulated in these immune pathways and could enhance phagocytosis directly or indirectly. Thus, phagocytosis was the main coelomic cellular immune response in *S. intermedius* challenged by spotting disease causative bacterium. The expression patterns of 10 DEGs were confirmed via RT-qPCR, and the expression levels were consistent with the results of RNA-seq. Furthermore, 9899 SSRs were identified, and 123,692, 151,827, and 114,368 candidate SNPs were identified from CG, DG, and UG, respectively. These results provide basic information for our understanding of sea urchin antibacterial immunity.

1. Introduction

The sea urchin *Strongylocentrotus intermedius* is originally found off the coast of North Japan and Far Eastern Russia and was introduced from Japan to China in 1989 [1]. *S. intermedius* has been exploited along the northern coast of the Yellow Sea in China in the last decades for its highly valued gonads [2]. To date, *S. intermedius* is the only large-scale long-line-cultured sea urchin species in China. Recently, the market demand for sea urchin has increased rapidly in large and developed cities in China. Thus, the aquaculture of *S. intermedius* plays an increasingly important role in mitigating the contradiction between market demand and the overfishing of natural sea urchin populations. However, the frequent outbreaks of diseases are constantly threatening sea urchin aquaculture. Infectious diseases lead to mass mortality occasionally in either juveniles in hatcheries or adults in aquaculture farms [3–9].

Spotting disease is a commonly observed disease in *S. intermedius* [3,4,7,9]. This disease outbreaks in summer when the water temperature exceeds 20 °C. The infected sea urchins have single or multiple spotting lesions with red, purple, or blackish color on the body wall

* Corresponding author. State Key Laboratory for Quality and Safety of Agro-products, Ningbo University, 818 Fenghua Road, Ningbo, Zhejiang Province, 315211, PR China.
** Corresponding author. Key Laboratory of Mariculture & Stock Enhancement in North China's Sea, Ministry of Agriculture and Rural Affairs, Dalian Ocean University, 52, Heishijiao Street, Dalian, Liaoning Province, 116023, PR China.
E-mail addresses: lichenghua@nbu.edu.cn (C. Li), yqchang@dlou.edu.cn (Y. Chang).

https://doi.org/10.1016/j.fsi.2019.10.002
Received 14 July 2019; Received in revised form 25 August 2019; Accepted 1 October 2019
Available online 01 October 2019
1050-4648/

followed by the detachment of local spines. The expansion of the lesions will cause ulceration on the test plates and finally lead to death. Two bacteria, namely, *Flexibacter* sp. and *Vibrio* sp., were recognized as the pathogen of spotting disease by Tajima et al. [4] and Wang et al. [8,9], respectively. Wang et al. [8] emphasized that extracellular products, such as casein and gelatinase of *Vibrio* sp., play a key role in causing spotting disease. We recently isolated a new causative bacterium from *S. intermedius* with spotting disease and identified that it belongs to the genus *Vibrio* but was different from the bacterium isolated by Wang et al. [9] (unpublished data). To date, the method through which the immune system works to protect the host from infection of spotting disease causative bacteria is rarely studied, although our previous study found that several important pathways are downregulated in individuals with spotting disease [10]. The host immune responses to causative bacteria of spotting disease in the sea urchin *S. intermedius* must be clarified to prevent and control spotting disease, especially to improve disease resistance via selective breeding.

In the present study, sea urchins were artificially infected using *Vibrio* sp. to obtain spotting diseased and undiseased samples. We constructed nine transcriptome libraries from coelomocytes of diseased, undiseased, and control *S. intermedius*. RNA-seq was subsequently performed using an Illumina Hiseq 4000 platform to examine the differences in immune-related gene expression. We aimed to clarify the signal transduction pathways involved in immune defense against the infection of the causative bacterium of spotting disease at the transcriptome level. This process might help us understand sea urchin antibacterial immunity and could be valuable for developing disease control strategy in aquaculture and in the selective breeding of sea urchins.

2. Materials and methods

2.1. Experimental bacteria and sea urchin

Pathogenic bacteria were isolated from the lesions of sea urchin with natural spotting disease in 2017 (described by our previous study [10]). One dominant bacterium (BAC1) was considered the pathogen of spotting disease in artificial infection experiment and was identified to belong to *Vibrio* (unpublished data). BAC1 was incubated for 14 h to the mid-logarithmic stage in 2216 E medium at 25 °C, harvested via centrifugation at 3500 rpm, and re-suspended to a final concentration of 1×10^7 colony-forming units mL^{-1} in phosphate-buffered saline (PBS) (NaCl 136.89 mM, KCl 2.67 mM, Na_2HPO_4 8.1 mM, KH_2PO_4 1.76 mM, pH 7.4). All of the experimental sea urchins were bred by Dalian Haibao Fishery, Co., Ltd. and cultured in longline in the Longwangtang sea area (38°48′38″ N, 121°23′51″ E) in Dalian, Liaoning Province, China. On October 30, 2018, 18 healthy specimens of *S. intermedius*, which are approximately 2 years old, with an average test diameter of 4.34 ± 1.77 cm and an average body weight of 33.81 ± 4.10 g were selected and transported to the Key Laboratory of Mariculture and Stock Enhancement in North China's Sea, Ministry of Agriculture and Rural Affairs, Dalian Ocean University. The sea urchins were maintained in 500 L aquarium tanks with flowing natural seawater for 2 weeks. The sea urchins were provided with the green algae *Ulva pertusa*. The water temperature was 16.0 °C ± 0.5 °C, pH was 8.2 ± 0.2, and salinity was 30.5 ± 0.5 ppt.

2.2. Challenge experiment and RNA preparation

Sea urchins were randomly divided into 2 groups: 14 individuals for the bacteria-challenged group and 4 individuals for the PBS CG. Sea urchins in the bacteria-challenged group were individually injected with 0.5 mL of BAC1 suspension, whereas individuals in the CG group were injected with 0.5 mL of PBS. Thereafter, the seven bacteria-challenged specimens and the four specimens in CG were separately cultured in three 100 L tanks. Seawater was heated from 16 °C to 23 °C in 7 days (1 °C per day) and maintained at 23 °C until the end of the experiment to simulate the water temperature condition that promotes spotting disease outbreaks. The experimental sea urchins in each tank were fed with *Ulva lactuca* pre-washed with sand-filtered seawater. The seawater in each tank was completely changed once every 3 days with sand-filtered seawater pre-heated to the same temperature. At 12 days after injection, 11 individuals in the bacteria-challenged group showed typical symptoms of spotting disease (Fig. 1), and they were assigned under the diseased group (DG). The three individuals that did not show any spotting disease lesions were assigned to the undiseased group (UG). The coelomic fluid of each specimen was collected and centrifuged immediately at 1000 × *g* for 10 min at 4 °C to harvest the coelomocytes. The samples were snap-frozen in liquid nitrogen immediately and then stored at −80 °C.

Fig. 1. Spotting disease lesion occurrence after BAC1 infection.

Total RNA was extracted using a Trizol reagent (Invitrogen, CA, USA) following the manufacturer's instruction. The RNA quantity and purity were analyzed using a Bioanalyzer 2100 and an RNA 1000 Nano LabChip kit (Agilent, CA, USA) with RIN number > 7.0.

2.3. cDNA library construction and sequencing

A specimen with single-value coelomocyte concentration within each group was recognized as abnormal and was not used for cDNA library construction. One and three specimens were discarded in the CG and DG, respectively. The specimens and their RNA levels in each experimental group for the cDNA library construction are listed in Table 1. The poly(A) mRNA from the samples of each group was isolated with poly-T oligo-attached magnetic beads using two rounds of purification. Then, mRNA was fragmented into small pieces using

Table 1
cDNA library construction method.

Experimental group	Library name	Containing specimens	RNA amounts per specimens (μg)	RNA amounts per library (μg)
CG	CG-1	CG-1	10	10
	CG-2	CG-2	10	10
	CG-3	CG-3	10	10
DG	DG-1	DG-1	3.33	10
		DG-2	3.33	
		DG-3	3.33	
	DG-2	DG-4	3.33	10
		DG-5	3.33	
		DG-6	3.33	
	DG-3	DG-7	5	10
		DG-8	5	
UG	UG-1	UG-1	10	10
	UG-2	UG-2	10	10
	UG-3	UG-3	10	10

divalent cations under elevated temperature. The cleaved RNA fragments were reverse-transcribed to create the final cDNA library in accordance with the protocol for an mRNA-Seq sample preparation kit (Illumina, San Diego, USA). The average insert size for the paired-end libraries was 300 bp (± 50 bp). Then, paired-end sequencing was performed on an Illumina Hiseq 4000 at the LC Sciences (USA) following the vendor's recommended protocol.

2.4. Transcriptome assembly

First, Cutadapt [11] and Perl scripts in house were used to remove the reads that contained adaptor contamination, low-quality bases, and undetermined bases. Second, sequence quality, including the Q20, Q30, and GC-content of the clean data, was verified using FastQC (http://www.bioinformatics.babraham.ac.uk/projects/fastqc/). All of the downstream analyses were based on high-quality clean data. De novo assembly of the transcriptome was performed using Trinity 2.4.0 [12]. Trinity group transcripts were clustered on the basis of shared sequence content. Such a transcript cluster was loosely referred to as a “gene.” The longest transcript in the cluster was chosen as the “gene” sequence (UniGene).

2.5. Gene annotation

The assembled UniGenes were aligned against the non-redundant (Nr) protein database (http://www.ncbi.nlm.nih.gov/), gene ontology (GO) (http://www.geneontology.org), SwissProt (http://www.expasy.ch/sprot/), Kyoto Encyclopedia of Genes and Genomes (KEGG) (http://www.genome.jp/kegg/), and eggNOG (http://eggnogdb.embl.de/) databases using DIAMOND [13] with a threshold of E-value < 0.00001.

2.6. Differential expression analysis

Salmon [14] was used to determine the expression levels of UniGenes by calculating TPM [15]. The differentially expressed UniGenes were selected with log2 (fold change) > 1 or log2 (fold change) < -1 and with statistical significance (P value < 0.05) using the R package edgeR [16]. GO and KEGG enrichment analyses were again performed on differentially expressed UniGenes using Perl scripts in house.

2.7. Validation of differentially expressed genes (DEGs) via RT-qPCR

Ten DEGs were selected for RT-qPCR validation (Table 2). RNA samples used for RT-qPCR amplification were the same as those used to construct the cDNA library. On the basis of the transcriptome sequences, the gene-specific primers were designed using Primer Premier 5.0 and are listed in Table 2. DEG analysis was performed using an ABI 7500 real-time PCR detection system. Real-time PCR amplification was performed in a 20 μL reaction containing 10 μL of 2 × SYBR Green Mix (TaKaRa), 2 μL of diluted cDNA (1:5), 0.8 μL of each primer (10 mM), 0.4 μL of ROX, and 6 μL of H_2O. The following qPCR parameters were used: (1) denaturing step at 95 °C for 5 min; (2) 40 cycles of 95 °C for 5 s, and (3) 60 °C for 32 s. The relative quantities of the target genes were calculated using β-actin from *S. intermedius* as an endogenous control gene in accordance with the $2^{-\triangle\triangle C_T}$ method [17].

2.8. Discovery of SSR and SNP

MISA software (http://pgrc.ipk-gatersleben.de/misa/) was used to detect putative SSRs from the assembled transcriptome. The parameters were adjusted to identify mono-, di-, tri, tetra-, penta-, and hexa-nucleotide motifs with a minimum of 12, 6, 5, 5, 4, and 4 repeats, correspondingly. The candidate SNPs were analyzed with the Bowtie software.

3. Results

3.1. Sequencing and UniGene assembly

Nine *S. intermedius* cDNA libraries with three CGs, three DGs, and three UGs were constructed. A total of 463, 416, 308 raw reads were obtained using the Illumina Hiseq 4000 system. After discarding the low-quality reads, 454, 139, 494 clean reads were obtained and used for de novo assembly (Table 3). The high-quality reads were deposited in the short-read archive of NCBI under the accession numbers SRR7701130, SRR7701131, SRR7701132, SRR7701133, SRR7701134, SRR7701135, SRR7701136, SRR7701137, and SRR7701138.

A total of 108,568 transcripts ranging from 201 bp to 33,255 bp with an N50 of 945 bp were assembled. A total of 23,899 UniGenes ranging from 201 bp to 33,255 bp with an N50 of 1359 bp were assembled (Table 4). The detailed length distribution of the transcripts is illustrated in Fig. 2.

Table 2
List of primers used for RT-qPCR validation.

Gene name (abbreviation)	Gene name (official full name)	Forward primer (5′-3′) and Reverse primer (5′-3′)	TM (°C)	Amplicon length (bp)
AGRN	serine protease inhibitor dipetalogastin-like	ACGAGAAGAACGCCGAGAG	57.4	203
		CGGGATGACACAACCAAAG	54.0	
CPA4	carboxypeptidase B-4	TTCCGTGTCACCCCTAAA	53.0	236
		GTCCCAGCCCTCTCCTCA	59.9	
nas-13	zinc metalloproteinase nas-13	AGATGGGTAAACGGTGTGG	54.7	295
		TTCGTGTCTGTTCGTGGTG	55.3	
ACE	angiotensin-converting enzyme	CGTTCCATACCCTGACCTACC	57.5	191
		CGTGACACACCACATCTCTCC	58.3	
cyb5r2	NADH-cytochrome b5 reductase 2-like	TGTGCCAGTGGTTGTAGG	55.0	181
		ACGGAAGCGACGGGTAT	56.6	
SI	sucrase-isomaltase, intestinal	GGCAGCATTCTTCCCTATCTTC	55.7	185
		GTCTAACCACTGTCCACCCATC	57.7	
Clec4g	C-type lectin lectoxin-Thr1	CCTGTTTCTCCTTGCCTCCA	57.5	280
		GCCTTCGTATTCCCTGTCATTT	55.0	
amy	alpha-amylase	ATCTCACCCCCTAATGAACACA	55.4	189
		CTCGTAAGACCAAGCAGCCA	57.6	
Selp	P-selectin-like	CGTTGTATCCTCCCCTCCTG	57.7	250
		TCCTATCCCGCTCTCCTGTC	58.7	
C3-pre	complement component C3 precursor	AGAATGGTGCTGTGAGGGTGC	60.7	120
		CCGTGATACTACTTGGAGTGGAGA	57.8	
β-actin	β-actin	AGAGGCGTAGAGGGAAAGAC	56.4	92
		ACAGGGAAAAGATGGCACAGA	56.4	

Table 3
Summary of the nine *S. intermedius* transcriptome.

Sample	Raw_Reads	Valid_Reads	Valid%
CG_1	55,621,500	54,900,502	98.70
CG_2	55,571,766	54,776,102	98.57
CG_3	47,779,884	47,088,752	98.55
DG_1	50,878,140	49,151,680	96.61
DG_2	52,471,666	51,479,712	98.11
DG_3	55,581,708	54,473,894	98.01
UG_1	49,868,700	48,786,118	97.83
UG_2	41,656,942	40,723,422	97.76
UG_3	53,986,002	52,759,312	97.73
Total	463,416,308	454,139,494	

Table 4
Basic information of assembled transcriptome.

Index	All	GC%	Min Length	Median Length	Max length	N50
Transcript	108,568	40	201	443	33,255	945
Gene	23,899	40	201	610	33,255	1359

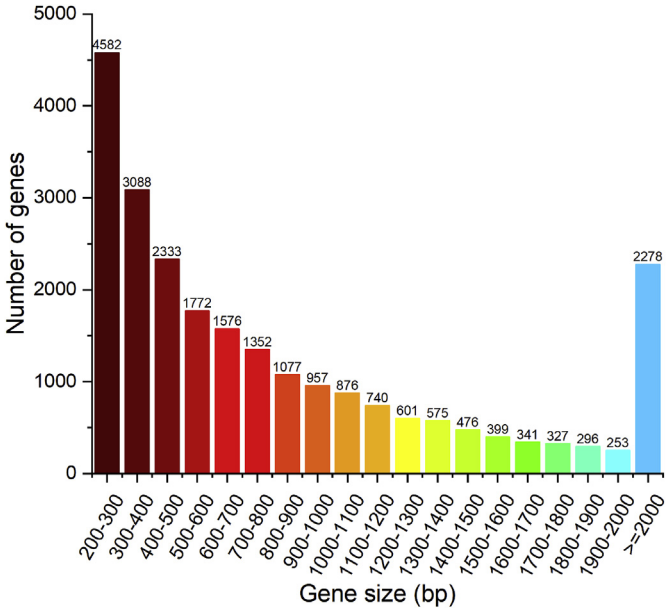

Fig. 2. Length distribution of assembled transcripts for all UniGenes.

3.2. Functional annotation of UniGenes

All of the UniGenes against GO, KEGG, Pfam, Swissprot, eggNOG, and Nr databases were conducted via the DIAMOND method. A total of 23,899 UniGenes had a significant hit on at least one target database (Table 5). The statistics of E-value, similarity, and target species for all Unigenes are presented in Fig. 3. The UniGenes with 0 E-value accounted for 7.12% of the total UniGenes. In the present study, 65.67% of the UniGenes had between 90% and 100% similarity with the target sequences. A total of 8415 UniGenes matched the Nr database, and most of them (86.11%) were aligned to the genome sequence of *S. purpuratus*, which belongs to the same genus of *Strongylocentrotus* with *S. intermedius*.

Table 5
Statistics of annotation results of Unigenes.

DB	Num	Ratio (%)
All	23,899	100
GO	6459	27.03
KEGG	4028	16.85
Pfam	5909	24.72
Swissprot	5016	20.99
EggNOG	9211	38.54
NR	8415	35.21

A total of 19,905 transcripts were annotated by GO analysis with one or more GO terms. All of the GO terms were divided into three subcategories: “biological process,” “cellular component,” and “molecular function” (Fig. 4). GO annotation showed that 5258, 5545, and 5370 UniGenes were assigned terms in the biological process, cellular component, and molecular function, respectively. Most biological process-related genes were involved in the biological process, translation, oxidation reduction, and transcription regulation, DNA-templated. Most cellular component-related genes were involved in the cytoplasm, nucleus, and integral components of the membrane. Most molecular function-related genes were involved in protein binding, structural constitution of ribosome, and poly(A) RNA binding.

KEGG categories were also analyzed to characterize the functions of transcripts. A total of 7929 transcripts were mapped to 307 pathways. The pathway maps showed that six KEGG categories (i.e., organismal systems, metabolism, human diseases, genetic information processing, environmental information processing, and cellular processes) were annotated in *S. intermedius* transcriptomes (Fig. 5). The most abundant UniGenes (2061) was associated with metabolic pathways. The next largest category was the genetic information processing pathway with 1324 UniGenes.

3.3. Analysis of DEGs

A total of 725 DEGs were found among CG, DG, and UG. Gene expression comparisons between DG and CG identified 155 DEGs, including 142 upregulated and 13 downregulated DEGs. Gene expression comparisons between UG and CG identified 246 DEGs, including 133 upregulated and 113 downregulated DEGs. Gene expression comparisons between UG and DG identified 324 DEGs, including 63 upregulated and 261 downregulated DEGs (Fig. 6). The distribution of DEGs and non-DEGs are plotted in Fig. 7. The heatmap analysis of hierarchical clustering was used to determine DEG profiles (Fig. 8).

3.4. GO and KEGG enrichment analysis of DEGs

GO and KEGG functional enrichment analyses were performed to identify the main molecular functions of the DEGs involved. The GO pathways that changed significantly between DG and CG, UG and CG, and UG and DG are listed in Supplementary Tables 1–3. The GO functional enrichment analysis of DEGs was classified into three categories, namely, biological process, cellular component, and molecular function. The level-3 GO terms in the three categories are depicted in Fig. 9. In DG versus CG GO enrichment, the transport, integral membrane component, and extracellular space were mostly enriched. In UG and CG, GO enrichment, an integral component of plasma membrane, proteinaceous extracellular matrix, and receptor activity were mostly enriched. In the UG versus DG, GO enrichment, extracellular space, integral membrane component, and cytoplasm were mostly enriched. The KEGG pathway analysis revealed that 37, 20, and 49 pathways were enriched in the DG versus CG, UG versus CG, and UG versus DG, respectively. A total of 72 pathways were significantly enriched in DEGs. In the DG versus CG, the KEGG enrichment, vitamin digestion and absorption, phagosome, protein digestion, and absorption pathways were mostly enriched. In the UG and CG, the KEGG enrichment, phagosome, peroxisome, and lysine degradation pathways were mostly enriched. In the UG versus DG, the KEGG enrichment, Wnt signaling pathway, phagosome, and Notch signaling pathway were mostly enriched (Fig. 10; Supplementary Tables 4–6).

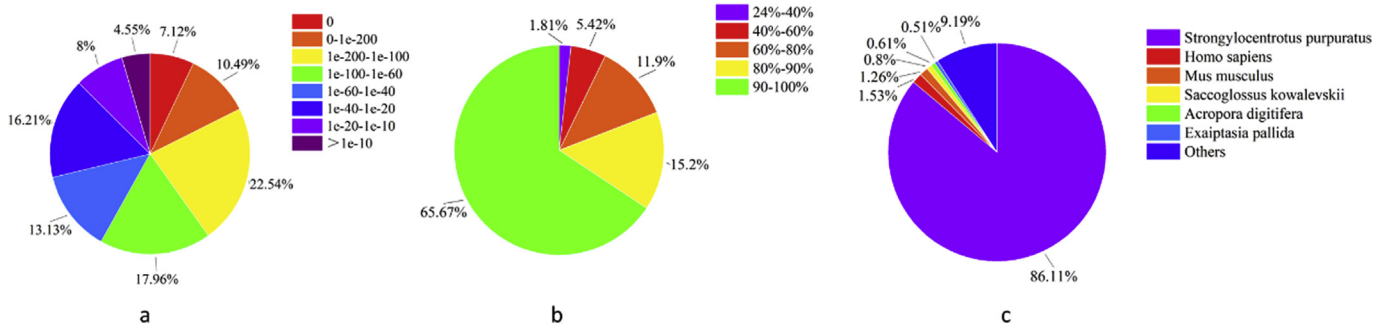

Fig. 3. Statistics of species with DIAMOND results in the Nr database. a: E-value distribution of BlastX hits with a cut-off E-value of 10^{-5}. b: Similarity distribution of the closest BlastX matches for each sequence. c: Species-based distribution of BlastX matches for sequences.

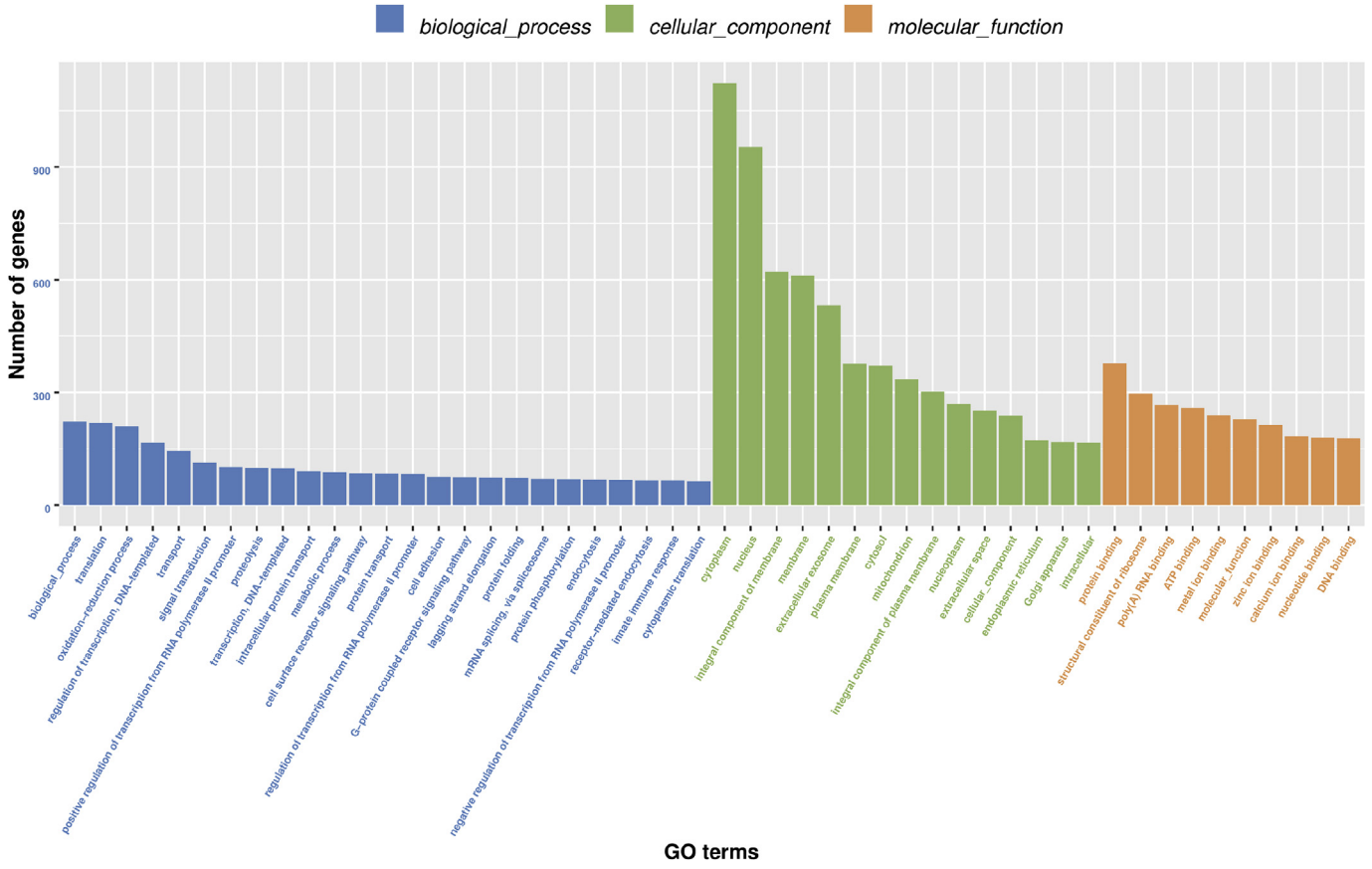

Fig. 4. Functional annotation of genes based on GO categorization.

3.5. RT-qPCR validation

We analyzed the expression of 10 genes, namely, serine protease inhibitor dipetalogastin-like (AGRN), carboxypeptidase B-4 (CPA4), nas-13, Cytb5r2, ACE, SI, C-type lectin lectoxin-Thr1 (Clec4g), amy, Selp, and complement component C3 precursor (C3-pre), from the transcriptome data using RT-qPCR to validate the DEGs identified by RNA-seq. Only one product was detected for each primer set via the dissolve curve analysis. The fold changes in DG versus CG and UG versus DG of RT-qPCR were compared with the RNA-seq expression profiles. All of the trends of RT-qPCR were correlated with the RNA-seq results, thereby indicating the reliability and accuracy of the assembly and RNA-seq expression analysis (Fig. 11).

3.6. Discovery of molecular markers

A total of 9899 SSRs were identified from the assembly sequences. The most abundant type of repeat motifs was mono-nucleotide repeats (5626), followed by di- (2708), tri- (1421), quad- (113), penta- (25), and hexa-nucleotide repeats (6) (Fig. 12). A total of 123,692, 151,817, and 114,368 candidate SNPs were identified from the CG, DG, and UG, correspondingly (Fig. 13). For the CG, 72,175 were transitions, and 51,517 were transversions. For the DG, 90,152 were transitions, and 61,665 were transversions. For the UG, 67,692 were transitions, and 46,676 were transversions. The numbers of A-G and C-T within the transition types were similar in all of the four groups. Within the transversion types, A-T was the most abundant, whereas C-G was the least for all of the four groups.

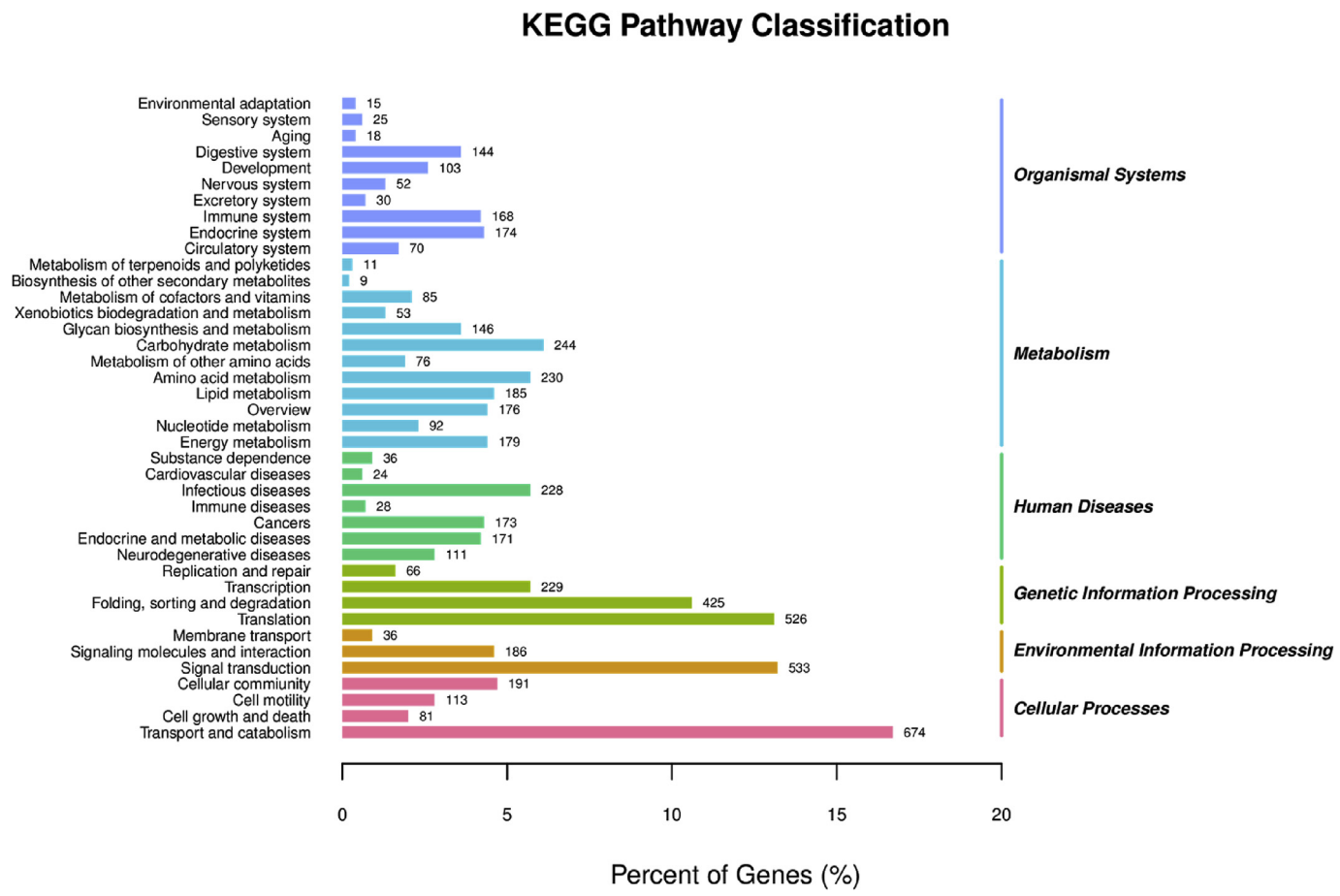

Fig. 5. Pathway enrichment of all annotated Unigenes via KEGG analysis.

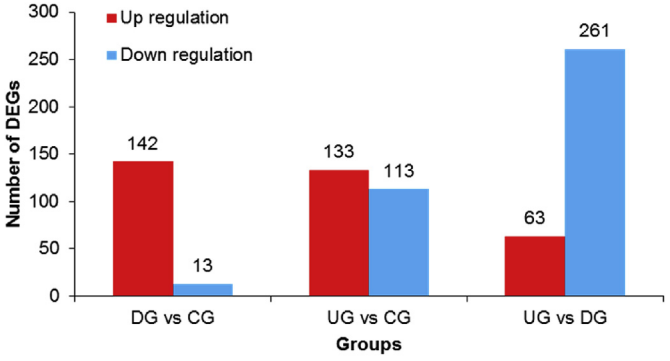

Fig. 6. Number of DEGs in the three comparison groups.

4. Discussion

In this study, 23,899 UniGenes were assembled with a minimum length of 201 bp, a maximum length of 33,255 bp, and an N50 of 1359 bp (Table 4). The number of UniGene is lower in the present study than in our previous study [10]; this result can be attributed to the upgraded overlap parameters from 10 bp to 20 bp during assembly. The goal is to reduce the probability of mismatch. Using this strategy, we obtained a UniGene number (23,899) that is close to the gene number of *S. purpuratus* genome (23,300) [18] and a long N50. This N50 is moderate in length among the results from other studies in *S. intermedius* [10,19,20]. In comparison with our previous work [10], the present study obtained large proportions of UniGenes that are longer than 2000 bp (9.53%) and between 500 and 2000 bp (48.62%) and a less proportion of UniGenes that are shorter than 500 bp. The proportion of UniGenes aligned to the genome sequences of *S. purpuratus* (86.11% of 8415 UniGenes) is comparable with previous studies in *S. intermedius* [10,19,20]. All of the abovementioned results suggest that the quality of transcriptome is high.

We aimed to clarify the genes involved in immune defense against infection from spotting disease at the transcriptome level. We successfully obtained diseased (DG) and undiseased (UG) samples via the artificial injection of the causative bacterium *Vibrio* sp. The gene expression comparisons between DG and CG, UG and CG, and UG and DG identified 155, 246, and 324 DEGs (Figs. 6 and 7), which account for 0.6%, 1.0%, and 1.4% of the total UniGenes, respectively. These proportions were lower than or comparable with our previous study (1.7%) [10]. However, more upregulated DEGs (142/155 in DG vs. CG) are present in artificially challenged sea urchins than naturally diseased sea urchins (689/1557) in the present study [10]. This difference could not be caused by the different infection methods because the injected BAC1 was the dominant bacterium isolated from individuals naturally infected with spotted disease. Moreover, another bacterium BAC2 was not dominant and could not cause spotting disease. This difference might be attributed to the different stages that experienced by the naturally diseased individuals and the artificially diseased ones. Spotting disease infection is a dynamic progression. The division method of progression of spotting disease can refer to that used in skin ulceration syndrome in sea cucumber *Apostichopus japonicus* [21]. In our previous study, diseased sea urchins with large lesions could belong to mid- or end-stage spotting disease, whereas, in the present study, the DG with small lesions could belong to early-stage spotting disease. Thus, the large proportion of upregulated DEGs in the DG in the present study indicated a positive immune response in *S. intermedius* during early-stage spotting disease. Most DEGs in the DG were upregulated in other

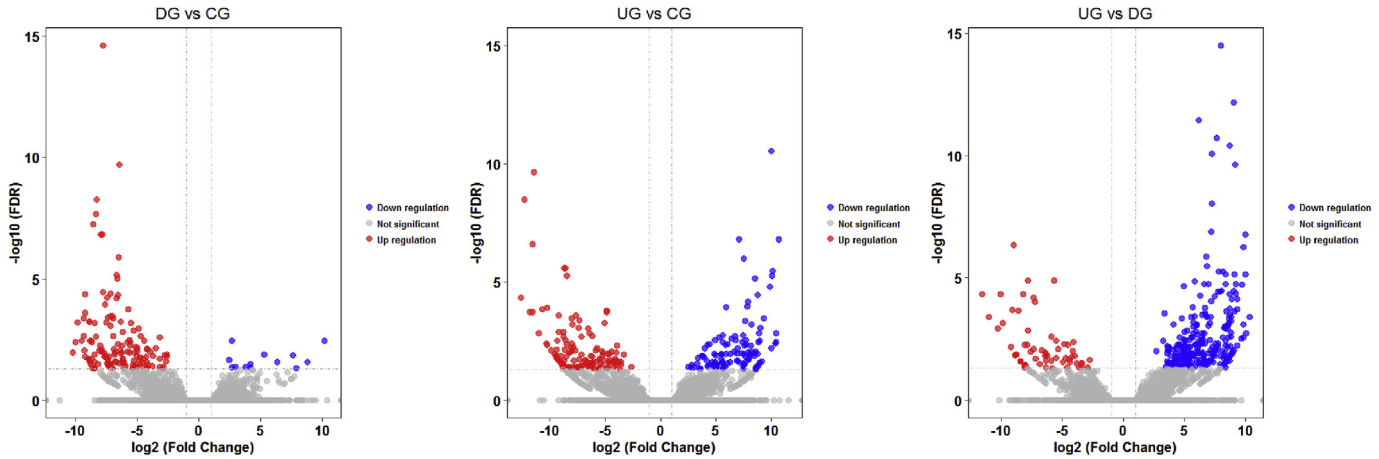

Fig. 7. DEG distribution between DG and CG, UG and CG, and UG and DG. log2 indicates the mean expression level for each gene. Each dot represents one gene. Blue and red dots represent DEGs. Gray dots represent the absence of DEGs (The interpretation of the references to color in this figure legend is available in the web version of this article). (For interpretation of the references to color in this figure legend, the reader is referred to the Web version of this article.)

aquatic animals, such as sea cucumber *A. japonicus* challenged with *Vibrio* sp. [21] and a backcross catfish progenies challenged with *Edwardsiella ictaluri* [22]. A total of 324 DEGs were observed in the UG versus the DG. These DEGs might include genes correlated with spotting disease resistant to a certain extent.

Several immune-related genes, such as C3-pre, complement C3, Clec4g, CPA4, and AGRN, were annotated. The DEG enrichment in the three comparison groups revealed several important pathways, such as the phagosome, peroxisome, Notch signaling, and Wnt signaling pathways (Fig. 10; Supplementary Tables 4–6). In these pathways, the phagosome pathway was also enriched in the sea urchins with naturally acquired spotting disease in our previous study [10], thereby suggesting that the phagosome pathway plays an important role in the immune process of *S. intermedius* as a defense to spotting disease. This phenomenon might explain the reason for phagocytic amebocytes accounting for more than 60% of the total coelomocytes [23] and provide evidence for the common view that phagocytosis is the major form of the antibacterial immunity in echinoderms [24–26]. Other pathways, such as the peroxisome, Notch signaling pathway, and Wnt signaling pathway were not enriched in sea urchins with natural spotting disease

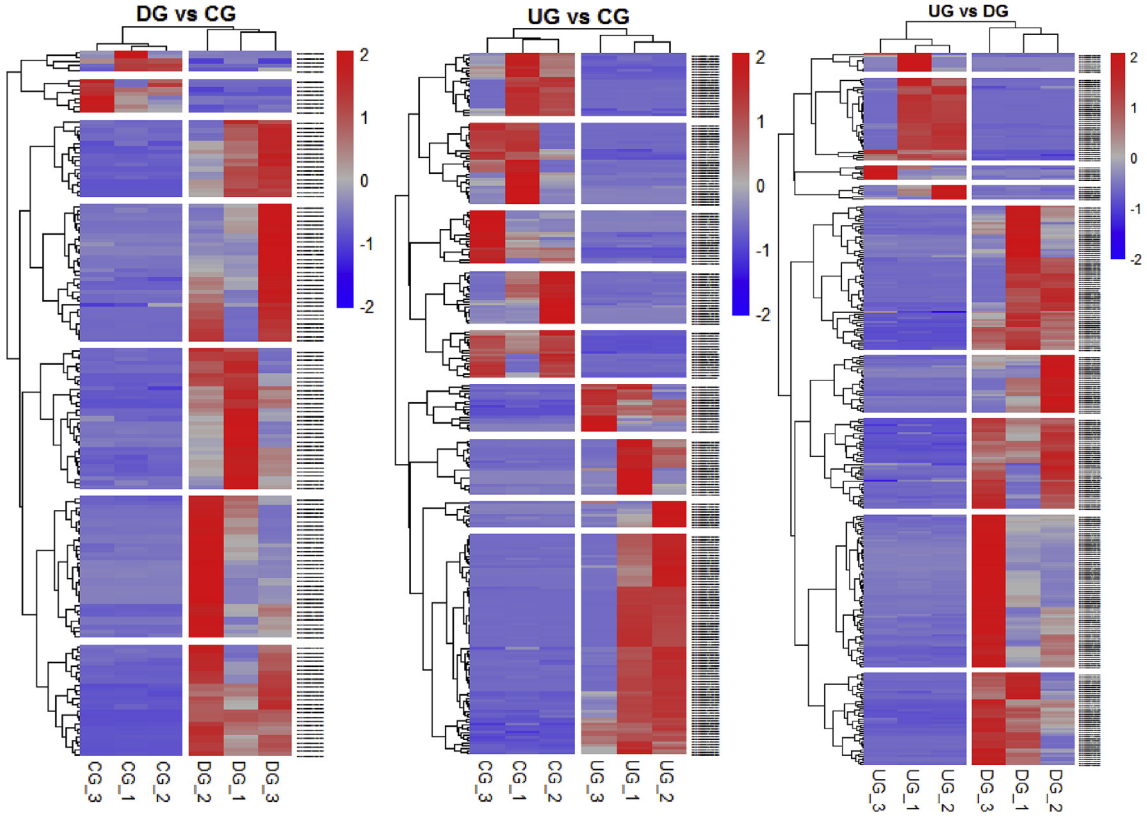

Fig. 8. Heatmap analysis of hierarchical clustering of DEGs in DG and CG, UG and CG, and UG and DG groups. Clusters were obtained via the hierarchical method based on 725 DEGs. Each column represents a CG, DG, or UG sample, and each row represents a gene. Different colors indicate differences in expression. Negative numbers mean downregulation, and positive numbers indicate upregulation. The high-definition figures were attached as Supplementary Figs. 1–3. (For interpretation of the references to color in this figure legend, the reader is referred to the Web version of this article.)

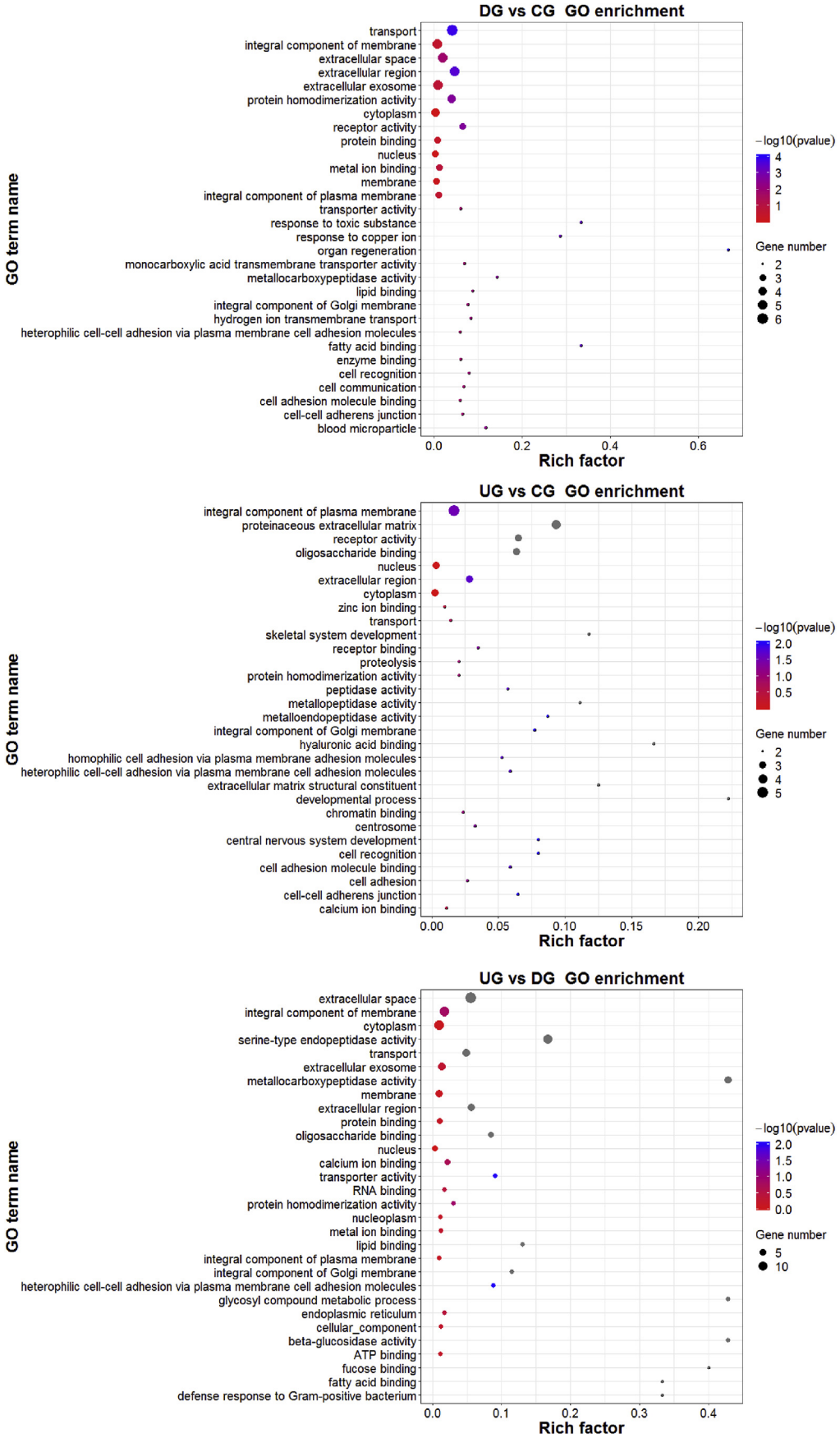

Fig. 9. GO enrichment of DEGs. The x-axis is the rich factor, which indicates the proportion of DEGs in total genes in a GO term. The y-axis is the gene functional classification of GO. Various colors of plots indicate different values of $-\log 10$ (*P* value). Plot diameter represents DEG numbers in a GO term. (For interpretation of the references to color in this figure legend, the reader is referred to the Web version of this article.)

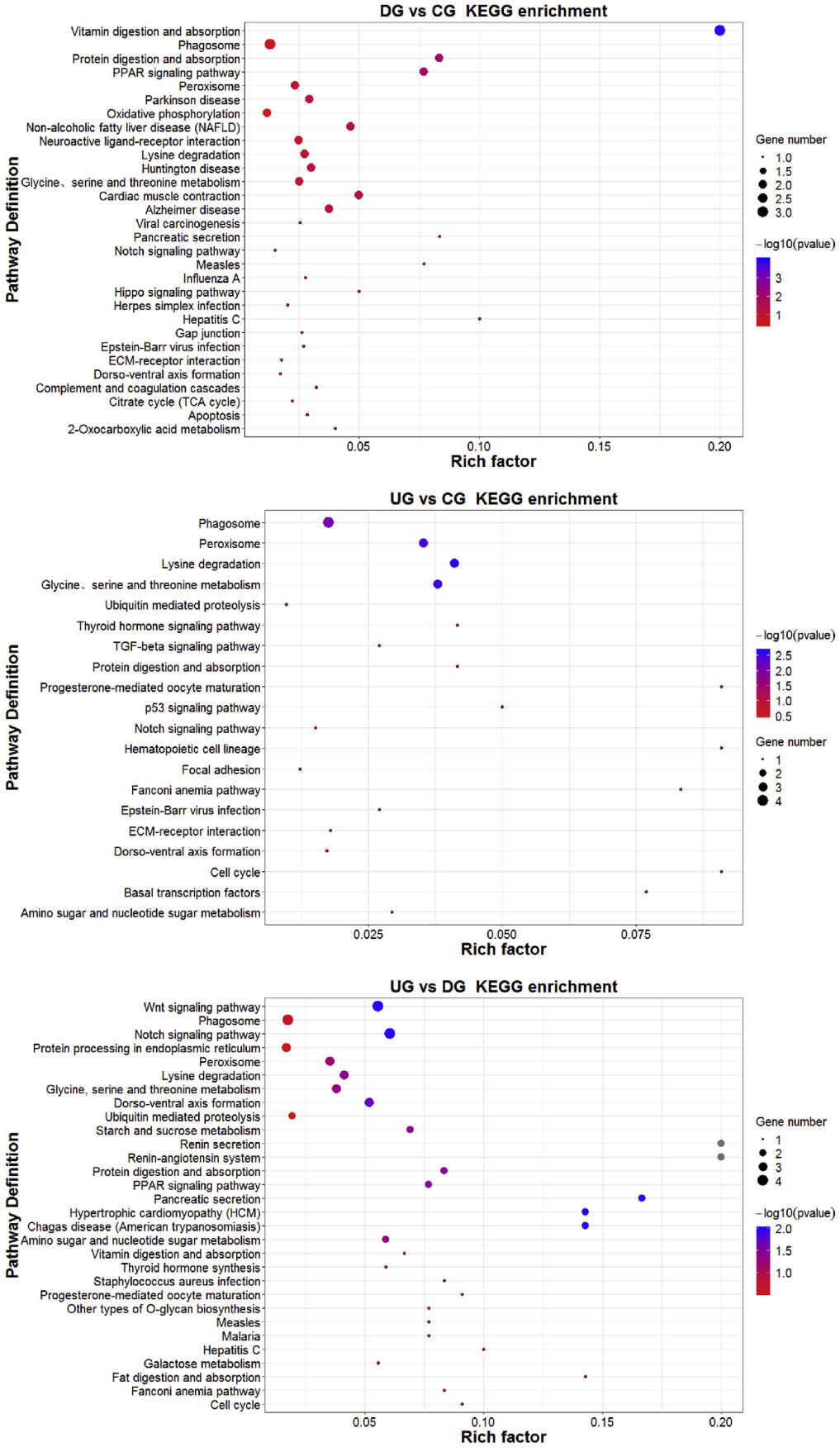

Fig. 10. KEGG enrichment of DEGs. The x-axis is the rich factor, which means that the proportion of DEGs in total genes in a KEGG term. The y-axis is the gene functional classification of KEGG. Various colors of plots indicate different values of −log 10 (*P* value). Plot diameter represents DEG numbers in a KEGG term. (For interpretation of the references to color in this figure legend, the reader is referred to the Web version of this article.)

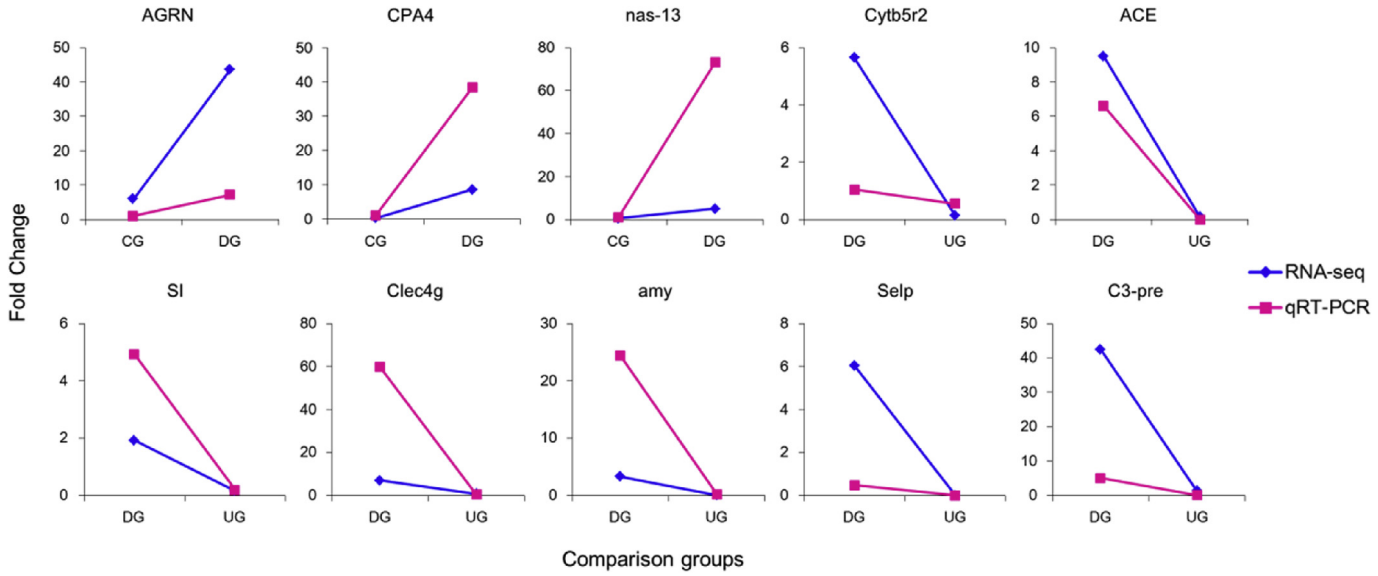

Fig. 11. Confirmation of DEG expression via RT-qPCR. Expression of the selected DEGs was normalized to that of the β-actin gene.

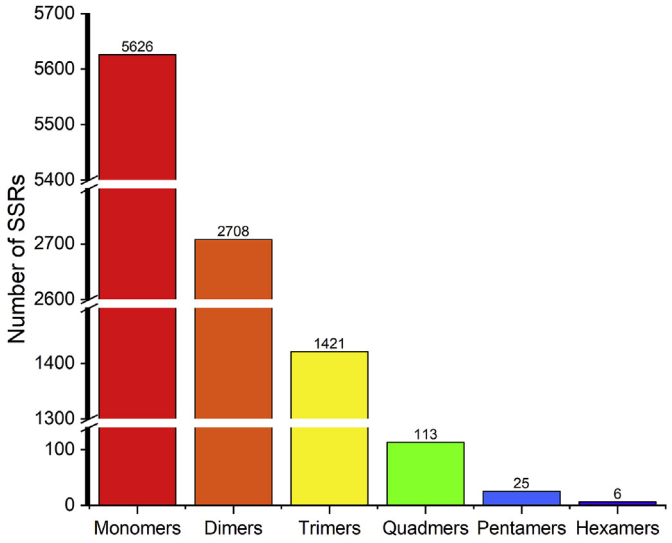

Fig. 12. Length distribution of SSRs based on the number of repeat units of *S. intermedius*. The x-axis is the SSR types.

[10], whereas the NOD-like receptor pathway and intestinal immune network for IgA production pathway were insignificantly enriched in the artificially infected ones. We demonstrated that the naturally diseased sea urchins in our previous study had mid- or end-stage spotting disease, and the artificially infected sea urchins in the present study had early-stage spotting disease. Thus, the immune system of *S. intermedius* might respond in accordance with the different strategies at various spotting disease infection stages.

In the present study, the phagosome pathway was significantly changed among the DG, UG, and CG. The gene expression of complement C3 and Clec4g was significantly upregulated in the DG and UG. C3 is the central component of the cascade and acts as an opsonin for pathogen phagocytosis and killing [26,27]. In sea urchin *S. purpuratus*, C3 promotes phagocytosis by physically tagging target cells for ingestion [28]. C-type lectin also shows opsonin functions with the ability to promote phagocytosis of coelomocytes in invertebrates [29,30]. The upregulated expression of C3 and Clec4g in bacterially challenged groups (DG and UG) indicated that *S. intermedius* augmented phagocytosis to kill the spotting disease causative bacterium *Vibrio* sp. The C3 and Clec4g expression level in the UG group was low, thereby suggesting that the phagocytosis function was downregulated in the UG. This phenomenon might be due to the injected bacteria that had been effectively controlled or cleared among undiseased individuals. This result was consistent with the result from Wang et al. [21] in catfish that is resistant to enteric septicemia. We reported the change in phagosome pathway in mid- or end-stage spotting disease [10]. The significant difference in phagosome pathway between the present and the previous studies were in the opposite regulation direction. This difference shows the manner through which the immune system changes when the spotting disease is aggravated. In early-stage spotting disease, sea urchins upregulated the function of phagocytosis, whereas, in the mid- or end-stage, they downregulated phagocytosis. The upregulation of phagocytosis in early-stage disease might be helpful for clearing the bacteria from the system and explain the reason that a self-cure phenomenon is occasionally observed in some spotting diseased individuals. The downregulation of the phagosome pathway in diseased sea urchin in the mid- or end-stage spotting disease could be a result of immune system exhaustion.

In comparison with the CG, the vitamin digestion and absorption pathways were promoted in the DG. Protein SpAN and blastula protease 10 (BP10) were upregulated. In mammals, SpAN and BP10 are secreted by the ileum and function as intrinsic factor (IF), which is essential to vitamin B_{12} digestion [31]. Vitamin B_{12} can maintain the hematopoietic function. Thus, the upregulated IF gene expression in diseased sea urchins was attributed to phagocytic amebocyte after killing *Vibrio* sp. It was essential to regenerate phagocytic amebocytes to maintain the stability of the immune system. This upregulation in the vitamin digestion and absorption pathway in diseased sea urchins indirectly enhanced their phagocytosis.

In comparison with DG, the function of the Wnt/Ca^{2+} pathway, which is a non-classical Wnt signaling pathway, was downregulated among sea urchins in the UG [32]. The Wnt signaling pathway was initially found to play critical roles in embryonic development and morphogenesis of animals [33]. An increasing number of studies have found that the Wnt signaling pathway was involved in stem cell differentiation and various diseases [34,35]. In the present study, four DEGs were enriched in the Wnt signaling pathway. They entered into K04515 orthology and belonged to calcium/calmodulin-dependent protein kinase II (CaM KII) family. CaM KII can enhance the proliferation of T cell and immune macrophages [36]; thus, the proliferation of coelomocytes among undiseased sea urchins may have been reduced. The proliferation of the coelomocytes among undiseased sea

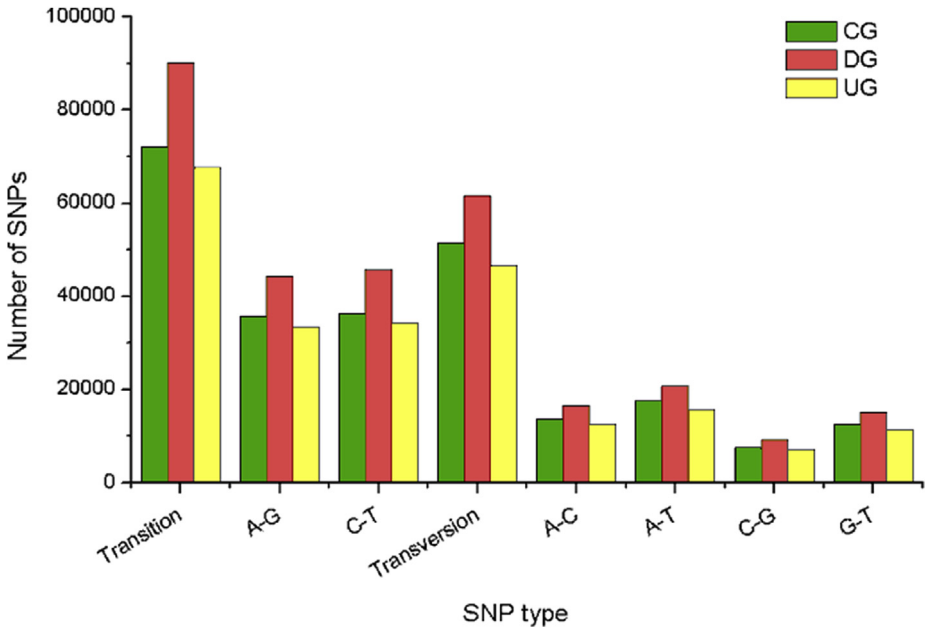

Fig. 13. Distribution of SNPs identified based on CG, DG, and UG in *S. intermedius*. The x-axis is the SNP type.

urchins might have been decreased via the Notch signaling pathway. The three DEGs that entered into the K 02599 orthology belonged to the Notch gene family downregulated their expression. The optimally characterized function of the Notch signaling pathway is its role in immunocytogenesis [37]. The function of the phagosome pathway among sea urchins in the UG was also downregulated as mentioned above. These downregulations in the UG suggested that the phagocytosis function among undiseased sea urchins was downregulated indirectly and directly. This phenomenon might also be due to the injected bacteria that had been effectively controlled or cleared. In comparison with the DG, 63 DEGs in the UG were upregulated and might contain genes correlated with disease resistance. However, most of them (49) failed to be annotated, and few could be used in the KEGG pathway enrichment. Annotations of the genome sequence are necessary to investigate genes or pathways involved in disease resistance in *S. intermedius*.

Abundant SSRs and SNPs were identified in the present study. More importantly, some SSRs and SNPs were located in the coding region or 5′-UTR or 3′-UTR of the DEGs including phagosome, vitamin digestion and absorption, Wnt signaling and Notch signaling pathways. Further studies should be conducted to reveal the relationship between these markers and disease resistance in *S. intermedius*, and it was expected that these SSRs and SNPs would play a tremendous role in marker-assisted selection for improving spotting disease resistance traits in *S. intermedius*.

In conclusion, we performed transcriptome-wide gene expression profiling of control, diseased, and undiseased *S. intermedius* challenged with *Vibrio* sp. and identified 725 DEGs. The reliability and accuracy of the assembly and RNA-seq expression analysis were confirmed via RT-qPCR results. Important immune pathways, such as phagosome, vitamin digestion and absorption, Wnt signaling pathway, and Notch signaling pathway were upregulated. These upregulations could enhance phagocytosis directly or indirectly. Consequently, phagocytosis should be the main coelomic cellular immune response in sea urchin *S. intermedius* challenged with the spotting disease causative bacterium and in early-stage disease. Our study clarified signal transduction pathways involved in antibacterial immunity at the transcriptome level. These data should be valuable to develop disease control strategy in aquaculture and selective breeding of sea urchins.

Notes

The authors declare no competing financial interest.

Acknowledgements

This work was financially supported by National Key R&D Program of China (Nos. 2018YFD0901601), a Grant for Chinese Outstanding Talents in Agricultural Research, and the K. C. Wong Magna Fund in Ningbo University.

Appendix A. Supplementary data

Supplementary data to this article can be found online at https://doi.org/10.1016/j.fsi.2019.10.002.

References

[1] Y. Chang, J. Ding, J. Song, et al., Biology and Aquaculture of Sea Cucumbers and Sea Urchins, Ocean press, Beijing, China, 2004, p. 217 (In Chinese).
[2] Y. Chang, Z. Wang, The raft culture of the sea urchin *Strongylocentrotus intermedius*, J. Dalian Fish. Univ. 12 (1997) 7–14 (In Chinese with English abstract).
[3] K. Tajima, T. Hirano, K. Nakano, et al., Taxonomical study on the causative bacterium of spotting disease of sea urchin *Strongylocentrotus intermedius*, Fisheries Sci. 63 (1997) 897–900.
[4] K. Tajima, T. Hirano, M. Shimizu, et al., Isolation and pathogenicity of the causative bacterium of spotting disease of sea urchin *Strongylocentrotus intermedius*, Fisheries Sci. 63 (1997) 249–252.
[5] K. Tajima, K. Takeuchi, I.M. Mahbub, et al., Studies on a bacterial disease of sea urchin *Strongylocentrotus intermedius* occurring at low water temperatures, Fisheries Sci. 64 (1998) 918–920.
[6] K. Takeuchi, K. Tajima, I.M. Mahbub, et al., Taxonomical and serological studies on the causative bacteria of the disease of sea urchin *Strongylocentrotus intermedius* occurring at low water temperatures, Fisheries Sci. 65 (1999) 264–268.
[7] Y. Wang, Y. Chang, J.M. lawrence, Disease in sea urchin, in: J.M. lawrence (Ed.), Sea Urchins: Biology and Ecology, 3 ed., Elsevier, United Kingdom, 2013, pp. 179–186.
[8] B. Wang, Y. Li, X. Li, et al., Pathogenic mechanism of the causative vibrio found in "red spotting" diseased sea urchin *Strongylocentrotus intermedius*, J. Dalian Fish. Univ. 20 (2005) 11–15 (in Chinese with English abstract).
[9] B. Wang, Y. Li, X. Li, et al., Biological characteristic and pathogenicity of the pathogenic vibrio on the "red spot disease" of *Strongylocentrotus intermedius*, J. Fish. China 30 (2006) 371–376 (in Chinese with English abstract).
[10] W. Zhang, Z. Lv, C. Li, et al., Transcriptome profiling reveals key roles of phagosome and NOD-like receptor pathway in spotting diseased *Strongylocentrotus intermedius*, Fish Shellfish Immunol. 84 (2019) 521–531.
[11] M. Martin, Cutadapt removes adapter sequences from high-throughput sequencing

reads, EMBnet J. 17 (2011) 10–12.
[12] M.G. Grabherr, B.J. Haas, M. Yassour, et al., Full-length transcriptome assembly from RNA-Seq data without a reference genome, Nat. Biotechnol. 29 (2011) 644–652.
[13] B. Buchfink, C. Xie, D.H. Huson, Fast and sensitive protein alignment using DIAMOND, Nat. Methods 12 (2015) 59.
[14] R. Patro, G. Duggal, M.I. Love, et al., Salmon provides fast and bias-aware quantification of transcript expression, Nat. Methods 14 (2017) 417–419.
[15] A. Mortazavi, B. Williams, K. McCue, et al., Mapping and quantifying mammalian transcriptomes by RNA-seq, Nat. Methods 5 (2008) 621.
[16] M.D. Robinson, D.J. Mccarthy, G.K. Smyth, edgeR: a Bioconductor package for differential expression analysis of digital gene expression data, Bioinformatics 26 (2010) 139.
[17] K. Livak, T. Schmittgen, Analysis of relative gene expression data using real-time quantitative PCR and the 2(-Delta Delta C(T)), Methods 25 (2001) 402–408.
[18] E. Sodergren, G.M. Weinstock, E.H. Davidson, et al., The genome of the sea urchin *Strongylocentrotus purpuratus*, Science 314 (2006) 941–952.
[19] Y. Chen, Y. Chang, X. Wang, et al., De novo assembly and analysis of tissue-specific transcriptomes revealed the tissue-specific genes and profile of immunity from *Strongylocentrotus intermedius*, Fish Shellfish Immunol. 46 (2015) 723–736.
[20] J. Ding, D. Yang, Y. Chang, et al., Comparative transcriptome analysis of tube feet of different colors in the sea urchin *Strongylocentrotus intermedius*, Genes Genom 39 (2017) 1215–1225.
[21] A. Yang, Z. Zhou, Y. Pan, et al., RNA sequencing analysis to capture the transcriptome landscape during skin ulceration syndrome progression in sea cucumber *Apostichopus japonicus*, BMC Genomics 17 (2016) 459.
[22] R. Wang, L. Sun, L. Bao, et al., Bulk segregant RNA-seq reveals expression and positional candidate genes and allele-specific expression for disease resistance against enteric septicemia of catfish, BMC Genomics 14 (2013) 929.
[23] K. Bertheussen, R. Seljelid, Echinoid phagocytes in vitro, Exp. Cell Res. 111 (1978) 401–412.
[24] J.C.S. Borges, B.E. Jensch-Junior, P.A.G. Garrido, et al., Phagocytic amoebocyte sub populations in the perivisceral coelom of the sea urchin *Lytechinus variegatus* (Lamarck, 1816), J. Exp. Zool. A Comp. Exp. Biol. 303A (2005) 241–248.
[25] Y. Ren, Q. Li, Y. Wang, et al., Research advances on coelomocyte of Echinodermata, J. Agric. Sci. Technol. 21 (2019) 91–97.
[26] L.C. Smith, J.P. Rast, V. Brockton, et al., The sea urchin immune system, ISJ-Invert Surviv J. 3 (2006) 217–224.
[27] L.C. Smith, J. Ghosh, K.M. Buckley, et al., Echinoderm immunity, in: K. Söderhäll (Ed.), Invertebrate Immunity, Springer US, 2010, pp. 260–301.
[28] L.A. Clow, D.A. Raftos, P.S. Gross, et al., The sea urchin complement homologue, SpC3, functions as an opsonin, J. Exp. Biol. 207 (2004) 2147–2155.
[29] X. Wang, X. Zhao, J. Wang, C-type lectin binds to β-Integrin to promote hemocytic phagocytosis in an invertebrate, J. Biol. Chem. 289 (2014) 2405–2414.
[30] A.M. Kerrigan, G.D. Brown, C-type lectins and phagocytosis, Immunobiology 214 (2009) 562–575.
[31] S. Demir, A. Ogan, N. Kayaman-Apohan, Intrinsic factor and vitamin B12 complex-loaded poly[lactic-co-(glycolic acid)] microspheres: preparation, characterization and drug release, Polym. Int. 57 (2010) 372–377.
[32] M. Kühl, L.C. Sheldahl, M. Park, et al., The Wnt/Ca^{2+} pathway : a new vertebrate Wnt signaling pathway takes shape, Trends Genet. 16 (2000) 279–283.
[33] C. Guo, H. Fan, Research advance of the Wnt signaling in peripheral immunoregulation, Chin. Bull. Life Sci. 22 (2010) 357–361 (In Chinese with English abstract).
[34] M. Katoh, M. Katoh, Wnt signaling pathway and stem cell signaling network, Clin. Cancer Res. 13 (2007) 4042–4045.
[35] J.L. Song, P. Nigam, S.S. Tektas, et al., microRNA regulation of Wnt signaling pathways in development and disease, Cell. Signal. 27 (2015) 1380–1391.
[36] M.Y. Lin, T. Zal, Irene L. Ch'en, et al., A pivotal role for the multifunctional calcium/calmodulin-dependent protein kinase II in T cells: from activation to unresponsiveness, J. Immunol. 174 (2005) 5583–5592.
[37] I. Maillard, S.H. Adler, W.S. Pear, Notch and the immune system, Immunity 19 (2003) 781–791.